The loss of both pUL16 and pUL21 in HSV-1 infected cells abolishes cytoplasmic envelopment.

Kellen Roddy[1], Peter Grzesik[1], Barbara Smith[2], Nathan Ko[1], Sanjay Vashee[3] and Prashant J. Desai[1,*]

[1] Department of Oncology, [2] Department of Cell Biology, Johns Hopkins University School of Medicine, Baltimore and [3] Synthetic Biology and Bioenergy, J. Craig Venter Institute, Rockville, MD, USA.

*Correspondence: pdesai@jhmi.edu (PJD) Tel: (410) 614-1581 (PJD)

Abstract

Previously, we had developed synthetic genomics methods to assemble an infectious clone of herpes simplex virus type-1 (HSV-1). To do this, the genome was assembled from 11 separate cloned fragments in yeast using transformation associated recombination. The eleven fragments or “parts” spanned the 152 kb genome and recombination was achieved because of the overlapping homologous sequences between each fragment. To demonstrate the robustness of this genome assembly method for reverse genetics, we engineered different mutations that were located in distant loci on the genome and built a collection of HSV-1 genomes that contained single and different combination of mutations in 5 conserved HSV-1 genes. The five genes: UL7, UL11, UL16, UL21 and UL51 encode virion structural proteins and have varied functions in the infected cell. Each is dispensable for virus replication in cell culture, however, combinatorial analysis of deletions in the five genes revealed “synthetic-lethality” of some of the genetic mutations. Thus, it was discovered that any virus that carried a UL21 mutation in addition to the other gene was unable to replicate in Vero cells. Replication was restored in a complementing cell line that provided pUL21 in trans. One particular combination (UL16-UL21) was of interest because the proteins encoded by these genes are known to physically interact and are constituents of the tegument structure. Furthermore, their roles in HSV-1 infected cells are unclear. Both are dispensable for HSV-1 replication, however, in HSV-2 their mutation results in nuclear retention of assembled capsids. We thus characterized these viruses that carry the single and double mutant. What we discovered is that in cells where both pUL16 and pUL21 are absent, cytoplasmic capsids were evident but did not mature into enveloped particles. The capsid

particles isolated from these cells showed significantly lower levels of incorporation of both VP16 and pUL37 when compared to the wild-type capsids. These data now show that of the tegument proteins, like the essential pUL36, pUL37 and VP16; the complex of pUL16 and pUL21 should be considered as important mediators of cytoplasmic maturation of the particle.

Keywords: Herpes simplex virus, tegument proteins, pUL16, pUL21, cytoplasmic envelopment.

INTRODUCTION

Herpesvirus genomes have the coding capacity in excess of 100 genes. Many of these gene products have functions that are clearly defined as to their roles in virus replication. However, there are several gene products, many of them structural components of the virion, whose functions and activities in infected cells remain a mystery and have yet to be completely elucidated.

The herpes simplex virus type-1 (HSV-1) virion is comprised of four structural components: an icosahedral capsid, which encloses the viral DNA genome; an electron dense asymmetrically distributed material, which immediately surrounds the capsid and is termed the tegument; and an outer membrane or envelope, which encloses the tegument and capsid and in which are embedded the viral glycoproteins [1-4]. Capsid assembly and DNA packaging into icosahedral capsids are nuclear events. Subsequent nuclear exit and cytoplasmic envelopment, involve the participation of a large and diverse set of ~50 proteins.

The tegument is one of the most complex and diverse structures of the virion both in terms of protein composition and the functions encoded by the constituents of this structure. The tegument is comprised of a dense protein network that maintains this structure even when devoid of the virus envelope or capsid [5]. The virus specified polypeptides that comprise this structure include those that function to activate transcription, shut off host protein synthesis, uncoat the virus genome, phosphorylate virus proteins and others

whose functions are still poorly defined, reviewed in [4, 6-11]. The tegument displays a duality of functions in virus replication due to the role the proteins resident in this structure play both at early and at late times in infection. The tegument proteins have been classified as belonging to either the inner or outer layer of the tegument based on their close association with either the capsid (inner) or envelop (outer) [2, 12-16]. What has become increasingly evident is the importance of the tegument proteins in the maturation process of the enveloped virus. To date, three tegument proteins resident in the mature virion have been shown to have a deleterious and complete lethal effect on the maturation process. These are VP16 [17, 18], pUL36 (VP1/2) [19-22] and the product of the UL37 gene [20, 23, 24].

The studies presented here build on our recent experiments using the synthetic genomics assembly line to construct HSV-1 genomes carrying single, double, triple, quadruple and quintuplet mutations in different combinations (for the multiple mutations) of five genes encoding the tegument proteins pUL7, pUL51, pUL11, pUL16 and pUL21 [25]. This astonishing feat, to generate in parallel these mutant viruses, could only be done using this modular assembly method. Several studies have identified protein interactions between pUL7-pUL51 [26, 27] and between pUL11-pUL16-pUL21 [27-36] but other than single mutations, many have not been probed using multiple/combinatorial mutagenesis except for the UL7-UL51 gene pair [26, 37]. These proteins are conserved in all three of the herpesvirus families, yet are not essential, at least for HSV-1, in cell culture [26, 38-45]. They are most likely important for pathogenesis and spread of the virus *in vivo* as shown by analysis of some of the mutants in mouse model systems [46].

Our scientific premise is based on several lines of evidence that have demonstrated these proteins specify redundant functions because they are not required for virus replication in cell culture. We believe that we can uncover the nature of these "redundancies" using the novel synthetic genomics assembly line to discover "synthetic-lethals". To this end, we generated multiple HSV-1 genomes carrying different combinations of deletions in these five genes. The outcome of this investigation revealed that any mutant virus that carried a combination which included a deletion in the UL21 gene always displayed a lethal phenotype [25]. We further investigated the combination of UL16 and UL21 mutations because these proteins have a documented history of physical interactions in the infected cell [28, 30, 31]. The viruses carrying single mutations in these genes replicated in non-permissive cells albeit poorly. The double mutant virus displayed significant impairment in virus replication. When this virus was examined further, it was evident that the virus assembled DNA filled capsids and these particles were able to exit the nucleus but failed to acquire the envelop in the cytoplasmic compartment. Further examination of the DNA-filled C capsids revealed a significant reduction in the capsid association of VP16 (outer tegument) and pUL37 (inner tegument) proteins. This indicates that the pUL16-pUL21 complex is required for incorporation of these essential tegument proteins, revealing the complex nature of how HSV-1 capsids mature into infectious particles.

METHODS

Cells and Viruses

Vero cells and transformed Vero cell lines (G5-9) were all grown in minimal essential medium (alpha medium – Gibco Invitrogen) supplemented with 10% fetal bovine serum (FBS – Gibco Invitrogen) and passaged as described previously [47]. G5-9 is a subclone of the original G5 cell line isolated by Stan Person in 1993 [48]. This cell line carries a genomic fragment that includes UL16 and UL21 and thus complements mutants that carry deletions in these two genes. All stocks of HSV-1 viruses were amplified as also described by Desai et al. [47].

Antibodies

Antibodies to VP16 (LP1) were generated by Professor Tony Minson (University of Cambridge). This is a well characterized monoclonal antibody to this protein and has a significant citation record. Rabbit antibodies to pUL16 and pUL21 were made by John Wills (University of Pennsylvania, Hershey) and these have strong validation in the literature. Rabbit antibody to VP23 was generated by our lab using whole protein purified from capsid preparations and has demonstrated specificity [48]. Monoclonal antibody to gD (clone DL6) was generated by Dr. Cohen (University of Pennsylvania) and kindly provided to us by David Johnson (Oregon Health Sciences Center). This is a well-established antibody to gD. Antibody to pUL37 (rabbit polyclonal) was generated by Frank Jenkins (University of Pittsburgh). Mouse monoclonal antibody MCA406 which recognizes both VP21 and VP22a was purchased from Serotec Inc. GFP rabbit antibody (ab183734) was purchased from Abcam.

Cre excision

For the Cre excision, we used 2.5 μg of the DNA in a 50 μl volume reaction and used Cre enzyme (2 units/μl) (NEB). This was incubated at 37ºC for 30 minutes and then the enzyme heat-inactivated at 70ºC for 10 minutes. The whole 50 μl reaction was transfected into Vero or G5-9 cells using X-tremeGENE transfection reagent (Sigma-Aldrich) using the protocol previously [25]. The transfection was harvested 3 days post and sonicated to generate an infected cell lysate. This was serially diluted and used to infect cells in 96 well trays. Single plaques isolated were amplified and checked by Phire Hot Start II polymerase (Invitrogen) PCR assays to check for excision as described previously [25, 49]. Positives were amplified further to generate high titer working stocks.

Growth curves

Vero cells (5 x 10^5) in 12 well trays were either infected at a multiplicity of infection (MOI) of 0.01 or 10 plaque forming units (PFU)/ml. The cells were harvested at 24, 48 and 72 hours post-infection for the low MOI infections or at 24 hours post-infection for the high MOI infections. Cells were freeze/thawed three times and virus progeny titered on G5-9 monolayers.

Western blot analysis of infected cell lysates

Vero cells (5 x 10^5) were infected at an MOI of 10 PFU/cell and harvested 24 hours post infection. Cell pellets were lysed in 2X Laemmli buffer and 10% of this sample was resolved using Nu-Page 4-12% Bis-Tris gels (Invitrogen) and transferred to nitrocellulose membranes using the iBlot2 system (Invitrogen) as described by Luitweiler *et al*. [50].

Rabbit antibodies to HSV antigens were used at a dilution of 1:500. Blots were processed using the enhanced chemiluminescence (ECL) kit (GE Healthcare) or Clarity chemiluminescence kit (Bio-Rad) according the manufacturer's protocol and imaged using the iBright 1500 Imager (Invitrogen).

Fluorescence light microscopy imaging

For confocal imaging, RPE-1 cells (5 x 10^5) were seeded in a 4-well borosilicate glass bottom chamber slide (Lab-Tek). Cells were infected with each virus at a MOI of 10 PFU/cell and overlaid with FluroBrite DMEM (Thermo Fisher) supplemented with 1% FBS. 12 hours after infection, cells were imaged on a Zeiss LSM 510 confocal microscope using 63X objective.

Transmission electron microscopy (TEM)

Vero cells (5 x 10^5 cells) in 12 well tissue culture trays were infected at an MOI of 10 PFU/cell and processed for transmission electron microscopy (TEM) experiments [23]. Infected cells were processed 16 h post-infection. Samples were fixed in 2.5% glutaraldehyde, 3mM $MgCl_2$, in 0.1 M sodium cacodylate buffer, pH 7.2 for overnight at 4ºC. After buffer rinse, samples were postfixed in 1% osmium tetroxide in 0.1 M sodium cacodylate buffer (1 h) on ice in the dark. Following a DH_2O rinse and en bloc staining in 0.75% uranyl acetate for three hours, samples were dehydrated in a graded series of ethanol and embedded in Eponate resin overnight at 60ºC. Thin sections, 60 to 90 nm, were cut with a diamond knife on a Leica UltracutE ultramicrotome and picked up with 2x1 mm formvar coated copper slot grids. Grids were stained with 2% uranyl acetate

(aq.) and 0.4% lead citrate before imaging on a Hitachi 7600 TEM at 80 kV equipped with an AMT XR80 CCD.

Capsid purification and analysis of composition

Vero cells (20 X 10^6) in 100 mm tissue culture dishes were infected at an MOI of 5 and harvested after 24 h. Capsids from infected cells were released by treating infected cell pellets with 2x CLB [48] followed by 30 sec sonication. Next, capsids were separated using rate-velocity sedimentation on a 20-50% sucrose gradient. Capsid bands were visualized using light-scattering, and the C-capsid band was harvested by side-puncture. The capsid fractions were TCA precipitated and the pellets resuspended in 2X Laemmli sample buffer. Proteins were separated by SDS-PAGE on a NuPage 4-12% Bis-Tris gradient gels and stained using SYPRO Ruby stain according to the manufacturer's protocol (Thermo Fisher). Proteins from the same C-capsids preparations were again separated by SDS-PAGE and transferred to nitrocellulose membranes using the iBlot2 transfer machine. Membranes were processed for immunoblotting as described above. The primary antibodies used were rabbit R2421 αVP23 [48], mouse monoclonal LP1 for VP16 [51], rabbit 780 αUL37C [52], rabbit 74 αpUL16 [32], and rabbit 121 αpUL21 [31].

Quantitation of protein bands was performed using the iBright 1500 (Invitrogen). Bands were manually drawn and the values for Local Background Corrected Volume were calculated by the iBright software. For each set of C-Capsids, these values from the pUL37C and the VP16 bands were normalized to the Local Background Corrected

Volume value of VP23 from the same sample. The normalized values for each virus protein were then compared and analyzed using GraphPad Prism 9 software.

RESULTS

Cre excision of the BAC-YCp sequence in the mutant viruses

Previously, we had observed that the HSV-1 strain KOS yeast assembled genome had problems with replication in Vero cells. This was judged to be due to the presence of the BAC-YCp sequence in the virus genome. Removal of the sequence resulted in wild-type kinetics of virus replication [25]. Because we have the vector sequence bracketed by *loxP* sites we performed Cre-excision on all of our assembled genomes in order to remove the BAC-YCp element. We used an *in vitro* Cre excision method which gave us an efficiency of approximately 70% and more recently almost 90% [49]. Single plaques were isolated following transfection of cells and screened using PCR assays for excision of the vector sequence. These plaques were used to amplify the virus to obtain a secondary stock and subsequently high titer working stocks. All these viruses encode a VP16-Venus fusion protein which enables one to visually follow virus replication (Fig. 1a). This fusion does not affect the ability of the virus to replicate [25]. We typically passage all the mutant viruses in G5-9 cells because of the complementing activity provided *in trans*. G5 cells were transformed with the EcoR1 G fragment (HSV-1 KOS nucleotides 29281:45511) and pSV2neo [48]. This fragment encodes genes UL16 to UL21. This cell line can complement mutants in UL16, UL17, UL18, UL19, UL20 and UL21. G5-9 is a subclone of G5 that displays better complementing activity. When the mutant viruses were plaqued on Vero cells, the Δ16 and Δ21 mutant viruses gave rise to small plaques on Vero monolayers. Plaques were not observed on Vero cells when the double mutant virus was plated, only single fluorescent foci were observed (Fig. 1b).

235 **Protein expression**

236 We used rabbit antiserum against pUL16 and pUL21 to confirm the expression of these
237 proteins or their absence in cells infected with the different mutant viruses. Proteins
238 pUL16 (predicted mass 40 kD) and pUL21 (predicted mass 58 kD) were observed in cells
239 infected with the KOS^{YA} wild-type virus (Fig. 2). They were not observed in the cell lysates
240 of the corresponding mutant and both proteins were absent in the double Δ16/21 mutant
241 virus infected cells. We also examined the expression of other viral proteins in the same
242 lysates. Thus, the levels of gD, VP22a, pUL37 and VP16 looked similar in both the wild-
243 type and single mutant lysates. However, there was a detectable decrease in the levels
244 of protein accumulation in the double mutant.

245

246 **Growth curves**

247 In order to quantitate the growth defect in the different mutants, we performed growth
248 assays both at high multiplicity of infection (MOI) and at low MOI. Both the Δ16 and Δ21
249 mutant viruses could replicate on Vero cells but the yields of virus were lower than wild-
250 type virus infected cells. At low MOI, there was a 2 log reduction in virus yield (Fig. 3a)
251 and at high MOI there was a log reduction in virus titer (Fig. 4). For the double mutant
252 there was negligible virus growth. The low levels of virus detected correspond to the
253 amounts of input virus. This was also visually observed with the VP16 Venus fluorescence
254 in low MOI infections. The Δ16/21 mutant was completely unable to spread to neighboring
255 cells (Fig. 3b).

256

257

Confocal imaging of infected cells

Because the mutant viruses have the VP16-Venus tag in their genomes, we could visualize the fluorescence distribution using confocal light microscopy. For this, RPE-1 cells were used and infected at high MOI. Cells were imaged at 12h post-infection. VP16-Venus has a nuclear punctate distribution early in the infection but as time progresses, fluorescence is visualized at the nuclear and cytoplasmic membrane including the plasma membrane. In the cells infected with Δ16 mutant virus, the distribution of fluorescence was similar to wild-type. In the cells infected with Δ21 and Δ16/21 mutant viruses, the distribution of VP16 was perturbed and was less localized to the nuclear and cytoplasmic membranes. This was more evident for the double mutant virus (Fig. 5).

Ultrastructural analysis of infected cells

Vero cells were infected with all the mutant viruses and examined by electron-microscopy to visualize in greater detail what was happening within the cell (Fig. 6). For the wild-type infected cells, microscopy showed capsids in the nucleus, enveloped virus in the cytoplasm and at the cell surface, which is typical of productive virus production (Fig. 6a). In the cells infected with Δ16 (Fig. 6b) and Δ21 (Fig. 6c) mutant viruses, capsids were evident in the nucleus as well as in the cytoplasm. There were fewer enveloped viruses observed which reflects the lower production of virus in these cells. For the double mutant infected cells, we observed capsids in in the nucleus as well as in the cytoplasm (Fig. 6d). However, there were very few or no enveloped viruses detected in these cells.

281 **Capsid assembly**

282 We next examined capsid assembly and composition using purified capsids (Fig. 7).
283 Whole cell lysates were sedimented through sucrose gradients and all three capsid types
284 (A, B and C) were observed (Fig. 7a). There were lower levels of capsids in the gradients
285 using lysates for Δ16/21 infected cells as judged by light scatter. We extracted the C
286 capsids and analyzed these using total protein stain (Fig. 7b). One could readily identify
287 the major capsid proteins, however, the levels of these and thus C capsids was generally
288 also lower in the double mutant lysate gradients. We have analyzed a number of capsid
289 gradients following replicate infections. The experiment shown in (Fig. 7b) shows lower
290 levels of capsids in Δ16 virus cell lysates, which was not commonly seen. We next
291 examined these C capsids for their composition using available antibodies to the different
292 tegument and capsid proteins (Fig. 7c). We chose to normalize our capsids using
293 antibody to VP23 which is present in capsids in a fixed amount (600 copies). When
294 antibodies to VP16 and pUL37 were used, we observed a significant decrease in the
295 amounts detected relative to VP23 normalization. This was examined using the
296 quantitation software in the iBright 1500 and analyzed using GaphPad Prism9 software
297 (Fig. 7d). There was a significant reduction in the capsid association of both VP16 and
298 pUL37 in the mutant capsids. This same observation was observed in multiple replicate
299 analyses of C-capsids isolated from infected cells using the same methods.
300
301
302
303

DISCUSSION

Initial envelopment of the HSV-1 virion takes place at the inner nuclear membrane (INM). The interacting proteins, pUL31 and pUL34, the latter a membrane protein, are required for this initial envelopment; reviewed in [10, 11, 53-59] as well in some situations the US3 kinase. After the capsid is enveloped at the INM, it fuses with the outer nuclear membrane (ONM) depositing a naked (non-enveloped) particle into the cytoplasm [60]. These capsids are transported to the trans-Golgi compartment (TGN) or other cytoplasmic organelle (late endosomes) for final envelopment [10, 61-63]. This cytoplasmic site must accumulate all the different tegument proteins that are incorporated into the mature virion [4] and also the lipid membrane that envelopes this particle has to contain the full repertoire of viral glycoproteins, reviewed in [6, 10, 12, 56, 64-67]. One of the most intriguing aspects of this morphogenesis pathway is the role of the tegument proteins in this dual envelopment process, the cellular localization and movement of tegument proteins prior to their incorporation into the maturing virus and the viral factors/signals that traffic particles to the maturation compartment. What is still unclear is the composition of the tegument as the virus is translocated from the nucleus to the cell surface. The multitude of tegument proteins have different locations within the cell; some are exclusively cytoplasmic and others exclusively nuclear and yet others that are detected in both compartments. Thus, as the virus particle progresses on its way to the surface, all of these tegument components must be incorporated into the final mature virion. The mechanism by which it does this is still poorly understood. The manner by which protein-protein interactions determine the fate of virus particle formation is still unclear [6]. In fact

the tegument proteins appear to be required for the transition of the capsids from the site of assembly to the cytoplasmic site for final envelopment. Regardless most observations demonstrate the tegument primarily matures in the cytoplasm and sequential interactions between capsid-tegument, tegument-tegument and tegument-envelope drive the assembly of this structure [29, 68]. One of the key questions is what complex synthesizes the tegument assembly. Data has been interpreted that suggests [69-71] it is the largest tegument protein, pUL36 that initiates this. Data has also demonstrated the role of VP16 in complex with VP22, pUL41 and pUL47 as the “organizers” of the tegument [29, 70, 72-74]. Data has also implicated the complex comprised of pUL11, pUL16 and pUL21 playing a pivotal role in linking capsids with the envelope [28, 30-32, 35, 36, 75].

Clearly three tegument proteins, pUL36, pUL37 and VP16 are absolutely required for secondary envelopment. Additional gene products of the virus are also required, however, redundancy of activities in tissue culture may hide their distinct roles in this process. Proteins, pUL16 and pUL21 have been identified in different activities in the infected cell. The UL21 gene product has RNA binding activity, it is involved in syncytial processes, affects US3 kinase activity, inhibits innate immunity signaling, acts as a viral phosphatase and alters host metabolic pathways [76-82]. Protein UL16 similarly displays a variety of activities in the cell including interactions with host mitochondria [83, 84] as well as a role in syncytial formation [85]. Both pUL16 and pUL21 exhibit dynamic interactions with both tegument and glycoproteins of the virus [6, 28, 29, 32-35, 43, 85-88]. Deletion of each gene individually has been done in a number of HSV strains with differing results [40, 41, 43, 89-93]. In most cases, deletion of the gene in HSV-1 does not significantly affect virus

replication, albeit it can impact the levels of virus production. In HSV-2, the single deletion of UL16 or UL21, affects nuclear egress and retention of the viral genome in the assembled capsid [91, 94, 95]. Recent studies also demonstrate that a mutant with deletions in both UL16 and UL21 fails to dock to the nuclear pore [96]. These different activities illustrate the complexity of the functions of these two proteins in HSV infected cells. In our study in KOS HSV-1 strain, we do not see nuclear egress defects as judged by ultrastructural analyses but this could be due to strain differences between this family of viruses [93].

In our study, it is evident that pUL21 as well as pUL16 mediate important interactions that affect capsid association of tegument proteins. This includes the inner-tegument protein pUL37 and a major constituent of the tegument, VP16. The reduction of tegument protein incorporation affects robust virus replication (as in the case of the single deletions) or completely abolishes virus envelopment (as in the case of the double deletions). Both these proteins have extensive interactions with tegument and envelop proteins. pUL16 has been shown to interact with VP16 as well as gE, pUL11 and VP22 [28, 32-35, 43] and is required for the virion incorporation of gD [87]. Thus, the pUL16-pUL21 complex could be required for bridging interactions between the inner and outer teguments and subsequently with the envelop during secondary envelopment.

Author Contributions. KR, PG, BS, NK, SV and PD carried out the experiments. KR, PG, BS, NK, SV and PD wrote the manuscript and generated the figures.

Funding information

This work was supported by Public Health Service grant R01AI137365, R21AI109338, R03AI146632 and R01AI061382, from the National Institutes of Health.

Acknowledgements

We want to thank John Wills (Penn State Medical School) for antibodies to pUL16 and pUL21. Also, Professor Tony Minson (University of Cambridge) generously provided the LP1 monoclonal for our use. Finally, David Johnson (Oregon Health Sciences Center) and Frank Jenkins (University of Pittsburgh) for anti-gD and anti-pUL37 antibodies, respectively.

Conflicts of Interest

The authors declare that there are no conflicts of interest

FIGURE LEGENDS

Fig. 1. Illustration of the genotypes and phenotypes of the mutant viruses. (a) The genomes of the four viruses, WT (wild-type), Δ16, Δ21 and Δ16/21 (Δ:deletion) are shown. The deletions in the genes for UL16 and UL21 encompassed all the coding sequences. The Venus open reading frame (ORF) was fused to the C-terminus of VP16. Numbers of amino acid for each ORF are shown. (b) Fluorescence image of the plaquing efficiency of Δ16/21 on Vero and G5-9 cell lines (objective 10X).

Fig. 2. Expression of HSV-1 polypeptides in infected cells**.** Vero cells were synchronously infected with the indicated viruses or mock infected (MI). Cell lysates were collected 24 h post-infection and analyzed by SDS-PAGE and western blotting with antibodies for HSV-1 proteins. Both pUL16, or pUL21 are only observed in infected cell lysates for viruses expressing the corresponding wild-type gene. Additionally, lysates were probed with antibodies for gD, VP22a, pUL37, and VP16 which are all expressed with early and late gene kinetics and are unaltered in mutant virus lysates. Anti-VP16 antibodies detect the VP16-Venus fusion protein (92 kD).

Fig. 3. Viruses encoding deletions in UL16 and UL21 are attenuated for replication in Vero cells. (a) Vero cells were infected with each virus at a multiplicity of infection (MOI) of 0.01 plaque forming units (PFU)/cell and the infected cells harvested every 24 h over a 72 h period. Virus yield (PFU/mL) was enumerated by titration on G5-9 monolayers. Data from replicates was plotted for the multi-step growth curves. (b) Representative

410 images of Vero cells infected at an MOI of 0.01 PFU/cell from the same cultures as above
411 were obtained by fluorescence microscopy to visualize VP16-Venus expression at the
412 different times post-infection.
413
414 **Fig. 4.** Single-step growth curves of the mutant viruses. Vero cells were infected at an
415 MOI of 10 PFU/cell and the virus progeny harvested 24 h post-infection. Virus titers were
416 enumerated by plaquing on G5-9 cells. Data presented are representative of two
417 biological replicates.
418
419 **Fig. 5.** Confocal microscopy reveals disrupted perinuclear VP16-Venus localization in
420 infected cells lacking pUL21. RPE-1 cells were plated in chamber slides and
421 synchronously infected with each virus for 12 hours prior to live cell imaging by confocal
422 fluorescence microscopy to visualize VP16-Venus (objective 63X). Perinuclear VP16-
423 Venus was observed in WT virus and Δ16 infected cells, but this distribution became
424 irregular in either the Δ21 or Δ16/21 infected cells.
425
426 **Fig. 6.** Transmission electron microscopy shows enveloped capsids in single Δ16 or Δ21
427 null virus infected cells, but not in Δ16/21 infected cells. Vero cells were synchronously
428 infected with WT (a), Δ16 (b), Δ21 (c), or Δ16/21 (d) viruses (scale bar 1 μm) then fixed
429 16 h post-infection and processed for TEM imaging. Enveloped virus particles were
430 observed in the cytoplasm and egressing from WT infected cells (white arrows) and
431 observed at a lower frequency in Δ16 or Δ21 infected cells. Enveloped virus particles
432 were not observed in Δ16/21 cells and an accumulation of unenveloped capsids (white

433 arrowheads) was observed in the cytoplasm of these cells. The nucleus (n) and cytoplasm
434 (c) are marked.
435
436 **Fig. 7.** Isolation and analysis of mutant capsid particles. Vero cells were infected with
437 each virus (MOI=5) and infected cell pellets were collected 24 h post-infection. Capsids
438 from infected cells were released by treating infected cell pellets with 2X CLB and
439 sonication followed by separation of capsids on a 20-50% sucrose gradients and
440 ultracentrifugation. (a) Each capsid form — A, B, and C — are observed as light
441 scattering bands and denoted on the gradient images, each compared to the Δ16/21
442 capsid bands. (b) C-capsids were harvested by side puncture from each gradient and
443 proteins were separated by SDS-PAGE and observed by Sypro Ruby staining. Visible
444 capsid protein identities are indicated. (c) Proteins from the same C-capsids were again
445 separated by SDS-PAGE and probed for pUL16, or pUL21 by western blotting as well as
446 the capsid triplex protein VP23. Additionally, capsid proteins were also probed for inner-
447 tegument protein pUL37 or outer-tegument protein VP16 (Venus-fusion). (d) Quantitation
448 of levels of VP16 and pUL37 detected in the C-capsid fractions relative to the triplex
449 protein, VP23. Western blots were analyzed using the iBright 1500, yielding values of the
450 Local Background Corrected Volume for each protein band. The VP16 and pUL37
451 volumes were normalized to the VP23 volumes, and then normalized to the WT capsids.
452 Statistical analyses was performed with GraphPad Prism 9 using Student's *t*-test. ns: not
453 significant, P=<0.05 (*,**,***).
454
455

References

1. **Wildy P, Russell WC, Horne RW**. The morphology of herpes virus. *Virology* 1960;12:204-222.
2. **Grunewald K, Desai P, Winkler DC, Heymann JB, Belnap DM et al.** Three-dimensional structure of herpes simplex virus from cryo-electron tomography. *Science* 2003;302(5649):1396-1398.
3. **Dai X, Zhou ZH**. Structure of the herpes simplex virus 1 capsid with associated tegument protein complexes. *Science* 2018;360(6384).
4. **Loret S, Guay G, Lippe R**. Comprehensive characterization of extracellular herpes simplex virus type 1 virions. *J Virol* 2008;82(17):8605-8618.
5. **McLauchlan J, Rixon FJ**. Characterization of enveloped tegument structures (L particles) produced by alphaherpesviruses: integrity of the tegument does not depend on the presence of capsid or envelope. *J Gen Virol* 1992;73 (Pt 2):269-276.
6. **Owen DJ, Crump CM, Graham SC**. Tegument Assembly and Secondary Envelopment of Alphaherpesviruses. *Viruses* 2015;7(9):5084-5114.
7. **Smith GA**. Assembly and Egress of an Alphaherpesvirus Clockwork. *Adv Anat Embryol Cell Biol* 2017;223:171-193.
8. **Diefenbach RJ**. Conserved tegument protein complexes: Essential components in the assembly of herpesviruses. *Virus Res* 2015;210:308-317.
9. **Kelly BJ, Fraefel C, Cunningham AL, Diefenbach RJ**. Functional roles of the tegument proteins of herpes simplex virus type 1. *Virus Res* 2009;145(2):173-186.
10. **Crump C**. Virus Assembly and Egress of HSV. *Adv Exp Med Biol* 2018;1045:23-44.
11. **Ahmad I, Wilson DW**. HSV-1 Cytoplasmic Envelopment and Egress. *Int J Mol Sci* 2020;21(17).
12. **Mettenleiter TC, Klupp BG, Granzow H**. Herpesvirus assembly: an update. *Virus Res* 2009;143(2):222-234.
13. **Laine RF, Albecka A, van de Linde S, Rees EJ, Crump CM et al.** Structural analysis of herpes simplex virus by optical super-resolution imaging. *Nat Commun* 2015;6:5980.
14. **Zhou ZH, Chen DH, Jakana J, Rixon FJ, Chiu W**. Visualization of tegument-capsid interactions and DNA in intact herpes simplex virus type 1 virions. *J Virol* 1999;73(4):3210-3218.
15. **Cardone G, Newcomb WW, Cheng N, Wingfield PT, Trus BL et al.** The UL36 tegument protein of herpes simplex virus 1 has a composite binding site at the capsid vertices. *J Virol* 2012;86(8):4058-4064.
16. **Bohannon KP, Jun Y, Gross SP, Smith GA**. Differential protein partitioning within the herpesvirus tegument and envelope underlies a complex and variable virion architecture. *Proc Natl Acad Sci U S A* 2013;110(17):E1613-1620.
17. **Weinheimer SP, Boyd BA, Durham SK, Resnick JL, O'Boyle DR, 2nd**. Deletion of the VP16 open reading frame of herpes simplex virus type 1. *J Virol* 1992;66(1):258-269.
18. **Mossman KL, Sherburne R, Lavery C, Duncan J, Smiley JR**. Evidence that herpes simplex virus VP16 is required for viral egress downstream of the initial envelopment event. *J Virol* 2000;74(14):6287-6299.

19. **Desai PJ**. A null mutation in the UL36 gene of herpes simplex virus type 1 results in accumulation of unenveloped DNA-filled capsids in the cytoplasm of infected cells. *J Virol* 2000;74(24):11608-11618.
20. **Roberts AP, Abaitua F, O'Hare P, McNab D, Rixon FJ et al.** Differing roles of inner tegument proteins pUL36 and pUL37 during entry of herpes simplex virus type 1. *J Virol* 2009;83(1):105-116.
21. **Fuchs W, Klupp BG, Granzow H, Mettenleiter TC**. Essential function of the pseudorabies virus UL36 gene product is independent of its interaction with the UL37 protein. *J Virol* 2004;78(21):11879-11889.
22. **Schipke J, Pohlmann A, Diestel R, Binz A, Rudolph K et al.** The C terminus of the large tegument protein pUL36 contains multiple capsid binding sites that function differently during assembly and cell entry of herpes simplex virus. *J Virol* 2012;86(7):3682-3700.
23. **Desai P, Sexton GL, McCaffery JM, Person S**. A null mutation in the gene encoding the herpes simplex virus type 1 UL37 polypeptide abrogates virus maturation. *J Virol* 2001;75(21):10259-10271.
24. **Leege T, Granzow H, Fuchs W, Klupp BG, Mettenleiter TC**. Phenotypic similarities and differences between UL37-deleted pseudorabies virus and herpes simplex virus type 1. *J Gen Virol* 2009;90(Pt 7):1560-1568.
25. **Oldfield LM, Grzesik P, Voorhies AA, Alperovich N, MacMath D et al.** Genome-wide engineering of an infectious clone of herpes simplex virus type 1 using synthetic genomics assembly methods. *Proc Natl Acad Sci U S A* 2017;114(42):E8885-E8894.
26. **Albecka A, Owen DJ, Ivanova L, Brun J, Liman R et al.** Dual Function of the pUL7-pUL51 Tegument Protein Complex in Herpes Simplex Virus 1 Infection. *J Virol* 2017;91(2).
27. **Roller RJ, Fetters R**. The herpes simplex virus 1 UL51 protein interacts with the UL7 protein and plays a role in its recruitment into the virion. *J Virol* 2015;89(6):3112-3122.
28. **Han J, Chadha P, Starkey JL, Wills JW**. Function of glycoprotein E of herpes simplex virus requires coordinated assembly of three tegument proteins on its cytoplasmic tail. *Proc Natl Acad Sci U S A* 2012;109(48):19798-19803.
29. **Vittone V, Diefenbach E, Triffett D, Douglas MW, Cunningham AL et al.** Determination of interactions between tegument proteins of herpes simplex virus type 1. *J Virol* 2005;79(15):9566-9571.
30. **Meckes DG, Jr., Marsh JA, Wills JW**. Complex mechanisms for the packaging of the UL16 tegument protein into herpes simplex virus. *Virology* 2010;398(2):208-213.
31. **Harper AL, Meckes DG, Jr., Marsh JA, Ward MD, Yeh PC et al.** Interaction domains of the UL16 and UL21 tegument proteins of herpes simplex virus. *J Virol* 2010;84(6):2963-2971.
32. **Meckes DG, Jr., Wills JW**. Dynamic interactions of the UL16 tegument protein with the capsid of herpes simplex virus. *J Virol* 2007;81(23):13028-13036.
33. **Chadha P, Han J, Starkey JL, Wills JW**. Regulated interaction of tegument proteins UL16 and UL11 from herpes simplex virus. *J Virol* 2012;86(21):11886-11898.
34. **Loomis JS, Courtney RJ, Wills JW**. Binding partners for the UL11 tegument protein of herpes simplex virus type 1. *J Virol* 2003;77(21):11417-11424.

35. **Yeh PC, Han J, Chadha P, Meckes DG, Jr., Ward MD et al.** Direct and specific binding of the UL16 tegument protein of herpes simplex virus to the cytoplasmic tail of glycoprotein E. *J Virol* 2011;85(18):9425-9436.
36. **Yeh PC, Meckes DG, Jr., Wills JW**. Analysis of the interaction between the UL11 and UL16 tegument proteins of herpes simplex virus. *J Virol* 2008;82(21):10693-10700.
37. **Butt BG, Owen DJ, Jeffries CM, Ivanova L, Hill CH et al.** Insights into herpesvirus assembly from the structure of the pUL7:pUL51 complex. *Elife* 2020;9.
38. **Roller RJ, Haugo AC, Yang K, Baines JD**. The herpes simplex virus 1 UL51 gene product has cell type-specific functions in cell-to-cell spread. *J Virol* 2014;88(8):4058-4068.
39. **Fulmer PA, Melancon JM, Baines JD, Kousoulas KG**. UL20 protein functions precede and are required for the UL11 functions of herpes simplex virus type 1 cytoplasmic virion envelopment. *J Virol* 2007;81(7):3097-3108.
40. **Mbong EF, Woodley L, Frost E, Baines JD, Duffy C**. Deletion of UL21 causes a delay in the early stages of the herpes simplex virus 1 replication cycle. *J Virol* 2012;86(12):7003-7007.
41. **Baines JD, Koyama AH, Huang T, Roizman B**. The UL21 gene products of herpes simplex virus 1 are dispensable for growth in cultured cells. *J Virol* 1994;68(5):2929-2936.
42. **Baines JD, Roizman B**. The open reading frames UL3, UL4, UL10, and UL16 are dispensable for the replication of herpes simplex virus 1 in cell culture. *J Virol* 1991;65(2):938-944.
43. **Starkey JL, Han J, Chadha P, Marsh JA, Wills JW**. Elucidation of the block to herpes simplex virus egress in the absence of tegument protein UL16 reveals a novel interaction with VP22. *J Virol* 2014;88(1):110-119.
44. **Baines JD, Roizman B**. The UL11 gene of herpes simplex virus 1 encodes a function that facilitates nucleocapsid envelopment and egress from cells. *J Virol* 1992;66(8):5168-5174.
45. **Nozawa N, Kawaguchi Y, Tanaka M, Kato A, Kato A et al.** Herpes simplex virus type 1 UL51 protein is involved in maturation and egress of virus particles. *J Virol* 2005;79(11):6947-6956.
46. **Klopfleisch R, Klupp BG, Fuchs W, Kopp M, Teifke JP et al.** Influence of pseudorabies virus proteins on neuroinvasion and neurovirulence in mice. *J Virol* 2006;80(11):5571-5576.
47. **Desai P, DeLuca NA, Person S**. Herpes simplex virus type 1 VP26 is not essential for replication in cell culture but influences production of infectious virus in the nervous system of infected mice. *Virology* 1998;247(1):115-124.
48. **Desai P, DeLuca NA, Glorioso JC, Person S**. Mutations in herpes simplex virus type 1 genes encoding VP5 and VP23 abrogate capsid formation and cleavage of replicated DNA. *J Virol* 1993;67(3):1357-1364.
49. **Grzesik P, Ko N, Oldfield LM, Vashee S, Desai PJ**. Rapid and efficient in vitro excision of BAC sequences from herpesvirus genomes using Cre-mediated recombination. *J Virol Methods* 2018;261:67-70.
50. **Luitweiler EM, Henson BW, Pryce EN, Patel V, Coombs G et al.** Interactions of the Kaposi's Sarcoma-associated herpesvirus nuclear egress complex: ORF69 is a potent factor for remodeling cellular membranes. *J Virol* 2013;87(7):3915-3929.

51. **McLean C, Buckmaster A, Hancock D, Buchan A, Fuller A et al.** Monoclonal antibodies to three non-glycosylated antigens of herpes simplex virus type 2. *J Gen Virol* 1982;63(2):297-305.
52. **Shelton LS, Pensiero MN, Jenkins FJ**. Identification and characterization of the herpes simplex virus type 1 protein encoded by the UL37 open reading frame. *J Virol* 1990;64(12):6101-6109.
53. **Mettenleiter TC, Muller F, Granzow H, Klupp BG**. The way out: what we know and do not know about herpesvirus nuclear egress. *Cell Microbiol* 2013;15(2):170-178.
54. **Mettenleiter TC, Minson T**. Egress of alphaherpesviruses. *J Virol* 2006;80(3):1610-1611; author reply 1611-1612.
55. **Bigalke JM, Heuser T, Nicastro D, Heldwein EE**. Membrane deformation and scission by the HSV-1 nuclear egress complex. *Nat Commun* 2014;5:4131.
56. **Johnson DC, Baines JD**. Herpesviruses remodel host membranes for virus egress. *Nat Rev Microbiol* 2011;9(5):382-394.
57. **Reynolds AE, Ryckman BJ, Baines JD, Zhou Y, Liang L et al.** U(L)31 and U(L)34 proteins of herpes simplex virus type 1 form a complex that accumulates at the nuclear rim and is required for envelopment of nucleocapsids. *J Virol* 2001;75(18):8803-8817.
58. **Draganova EB, Thorsen MK, Heldwein EE**. Nuclear Egress. *Curr Issues Mol Biol* 2021;41:125-170.
59. **Roller RJ, Johnson DC**. Herpesvirus Nuclear Egress across the Outer Nuclear Membrane. *Viruses* 2021;13(12).
60. **Skepper JN, Whiteley A, Browne H, Minson A**. Herpes simplex virus nucleocapsids mature to progeny virions by an envelopment --> deenvelopment --> reenvelopment pathway. *J Virol* 2001;75(12):5697-5702.
61. **Sugimoto K, Uema M, Sagara H, Tanaka M, Sata T et al.** Simultaneous tracking of capsid, tegument, and envelope protein localization in living cells infected with triply fluorescent herpes simplex virus 1. *J Virol* 2008;82(11):5198-5211.
62. **Wisner TW, Johnson DC**. Redistribution of cellular and herpes simplex virus proteins from the trans-golgi network to cell junctions without enveloped capsids. *J Virol* 2004;78(21):11519-11535.
63. **Harley CA, Dasgupta A, Wilson DW**. Characterization of herpes simplex virus-containing organelles by subcellular fractionation: role for organelle acidification in assembly of infectious particles. *J Virol* 2001;75(3):1236-1251.
64. **Mettenleiter TC**. Budding events in herpesvirus morphogenesis. *Virus Res* 2004;106(2):167-180.
65. **Mettenleiter TC, Klupp BG, Granzow H**. Herpesvirus assembly: a tale of two membranes. *Curr Opin Microbiol* 2006;9(4):423-429.
66. **Lee GE, Church GA, Wilson DW**. A subpopulation of tegument protein vhs localizes to detergent-insoluble lipid rafts in herpes simplex virus-infected cells. *J Virol* 2003;77(3):2038-2045.
67. **Chi JHI, Harley CA, Mukhopadhyay A, Wilson DW**. The cytoplasmic tail of herpes simplex virus envelope glycoprotein D binds to the tegument protein VP22 and to capsids. *J Gen Virol* 2005;86(Pt 2):253-261.

68. **Lee JH, Vittone V, Diefenbach E, Cunningham AL, Diefenbach RJ**. Identification of structural protein-protein interactions of herpes simplex virus type 1. *Virology* 2008;378(2):347-354.
69. **Mijatov B, Cunningham AL, Diefenbach RJ**. Residues F593 and E596 of HSV-1 tegument protein pUL36 (VP1/2) mediate binding of tegument protein pUL37. *Virology* 2007;368(1):26-31.
70. **Svobodova S, Bell S, Crump CM**. Analysis of the interaction between the essential herpes simplex virus 1 tegument proteins VP16 and VP1/2. *J Virol* 2012;86(1):473-483.
71. **Ko DH, Cunningham AL, Diefenbach RJ**. The major determinant for addition of tegument protein pUL48 (VP16) to capsids in herpes simplex virus type 1 is the presence of the major tegument protein pUL36 (VP1/2). *J Virol* 2010;84(3):1397-1405.
72. **Elliott G, Mouzakitis G, O'Hare P**. VP16 interacts via its activation domain with VP22, a tegument protein of herpes simplex virus, and is relocated to a novel macromolecular assembly in coexpressing cells. *J Virol* 1995;69(12):7932-7941.
73. **Gross ST, Harley CA, Wilson DW**. The cytoplasmic tail of Herpes simplex virus glycoprotein H binds to the tegument protein VP16 in vitro and in vivo. *Virology* 2003;317(1):1-12.
74. **Smibert CA, Popova B, Xiao P, Capone JP, Smiley JR**. Herpes simplex virus VP16 forms a complex with the virion host shutoff protein vhs. *J Virol* 1994;68(4):2339-2346.
75. **Han J, Chadha P, Meckes DG, Jr., Baird NL, Wills JW**. Interaction and interdependent packaging of tegument protein UL11 and glycoprotein e of herpes simplex virus. *J Virol* 2011;85(18):9437-9446.
76. **Ma Z, Bai J, Jiang C, Zhu H, Liu D et al.** Tegument protein UL21 of alpha-herpesvirus inhibits the innate immunity by triggering CGAS degradation through TOLLIP-mediated selective autophagy. *Autophagy* 2023;19(5):1512-1532.
77. **Muradov JH, Finnen RL, Gulak MA, Hay TJM, Banfield BW**. pUL21 regulation of pUs3 kinase activity influences the nature of nuclear envelope deformation by the HSV-2 nuclear egress complex. *PLoS Pathog* 2021;17(8):e1009679.
78. **Sarfo A, Starkey J, Mellinger E, Zhang D, Chadha P et al.** The UL21 Tegument Protein of Herpes Simplex Virus 1 Is Differentially Required for the Syncytial Phenotype. *J Virol* 2017;91(21).
79. **Metrick CM, Heldwein EE**. Novel Structure and Unexpected RNA-Binding Ability of the C-Terminal Domain of Herpes Simplex Virus 1 Tegument Protein UL21. *J Virol* 2016;90(12):5759-5769.
80. **Takakuwa H, Goshima F, Koshizuka T, Murata T, Daikoku T et al.** Herpes simplex virus encodes a virion-associated protein which promotes long cellular processes in over-expressing cells. *Genes Cells* 2001;6(11):955-966.
81. **Benedyk TH, Connor V, Caroe ER, Shamin M, Svergun DI et al.** Herpes simplex virus 1 protein pUL21 alters ceramide metabolism by activating the interorganelle transport protein CERT. *J Biol Chem* 2022;298(11):102589.
82. **Benedyk TH, Muenzner J, Connor V, Han Y, Brown K et al.** pUL21 is a viral phosphatase adaptor that promotes herpes simplex virus replication and spread. *PLoS Pathog* 2021;17(8):e1009824.

83. **Chadha P, Sarfo A, Zhang D, Abraham T, Carmichael J et al.** Domain Interaction Studies of Herpes Simplex Virus 1 Tegument Protein UL16 Reveal Its Interaction with Mitochondria. *J Virol* 2017;91(2).
84. **Li S, Liu S, Dai Z, Zhang Q, Xu Y et al.** The UL16 protein of HSV-1 promotes the metabolism of cell mitochondria by binding to ANT2 protein. *Sci Rep* 2021;11(1):14001.
85. **Carmichael JC, Wills JW**. Differential Requirements for gE, gI, and UL16 among Herpes Simplex Virus 1 Syncytial Variants Suggest Unique Modes of Dysregulating the Mechanism of Cell-to-Cell Spread. *J Virol* 2019;93(15).
86. **DuRaine G, Wisner TW, Johnson DC**. Characterization of the Herpes Simplex Virus (HSV) Tegument Proteins That Bind to gE/gI and US9, Which Promote Assembly of HSV and Transport into Neuronal Axons. *J Virol* 2020;94(23).
87. **Carmichael JC, Starkey J, Zhang D, Sarfo A, Chadha P et al.** Glycoprotein D of HSV-1 is dependent on tegument protein UL16 for packaging and contains a motif that is differentially required for syncytia formation. *Virology* 2019;527:64-76.
88. **Nalwanga D, Rempel S, Roizman B, Baines JD**. The UL 16 gene product of herpes simplex virus 1 is a virion protein that colocalizes with intranuclear capsid proteins. *Virology* 1996;226(2):236-242.
89. **Muto Y, Goshima F, Ushijima Y, Kimura H, Nishiyama Y**. Generation and Characterization of UL21-Null Herpes Simplex Virus Type 1. *Front Microbiol* 2012;3:394.
90. **Le Sage V, Jung M, Alter JD, Wills EG, Johnston SM et al.** The herpes simplex virus 2 UL21 protein is essential for virus propagation. *J Virol* 2013;87(10):5904-5915.
91. **Gao J, Hay TJM, Banfield BW**. The Product of the Herpes Simplex Virus 2 UL16 Gene Is Critical for the Egress of Capsids from the Nuclei of Infected Cells. *J Virol* 2017;91(10).
92. **Finnen RL, Banfield BW**. CRISPR/Cas9 Mutagenesis of UL21 in Multiple Strains of Herpes Simplex Virus Reveals Differential Requirements for pUL21 in Viral Replication. *Viruses* 2018;10(5).
93. **Gao J, Yan X, Banfield BW**. Comparative Analysis of UL16 Mutants Derived from Multiple Strains of Herpes Simplex Virus 2 (HSV-2) and HSV-1 Reveals Species-Specific Requirements for the UL16 Protein. *J Virol* 2018;92(13).
94. **Gao J, Finnen RL, Sherry MR, Le Sage V, Banfield BW**. Differentiating the Roles of UL16, UL21, and Us3 in the Nuclear Egress of Herpes Simplex Virus Capsids. *J Virol* 2020;94(13).
95. **Thomas ECM, Bossert M, Banfield BW**. The herpes simplex virus tegument protein pUL21 is required for viral genome retention within capsids. *PLoS Pathog* 2022;18(11):e1010969.
96. **Thomas ECM, Finnen RL, Mewburn JD, Archer SL, Banfield BW**. The Herpes Simplex Virus pUL16 and pUL21 Proteins Prevent Capsids from Docking at Nuclear Pore Complexes. *PLoS Pathog* 2023;19(12):e1011832.

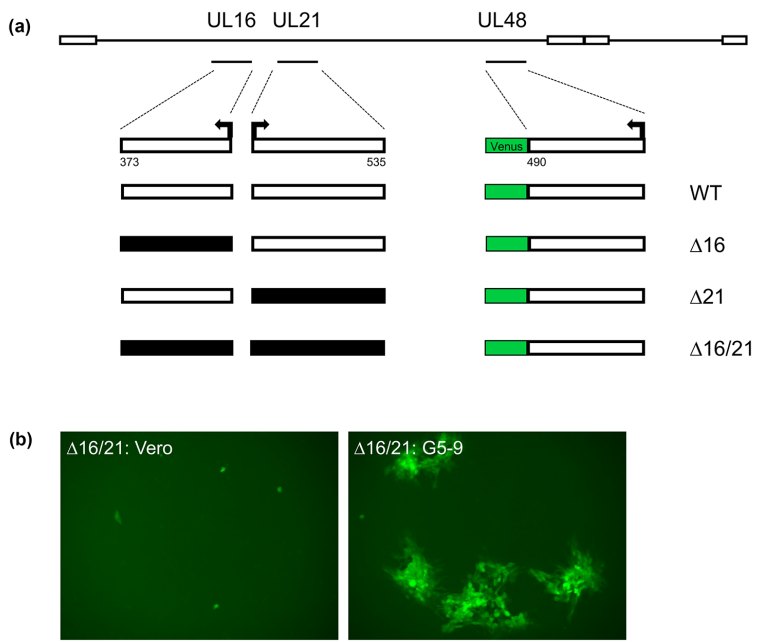

Fig. 1. Illustration of the genotypes and phenotypes of the mutant viruses. (a) The genomes of the four viruses, WT (wild-type), Δ16, Δ21 and Δ16/21 (Δ:deletion) are shown. The deletions in the genes for UL16 and UL21 encompassed all the coding sequences. The Venus open reading frame (ORF) was fused to the C-terminus of VP16. Numbers of amino acid for each ORF are shown. (b) Fluorescence image of the plaquing efficiency of Δ16/21 on Vero and G5-9 cell lines (objective 10X).

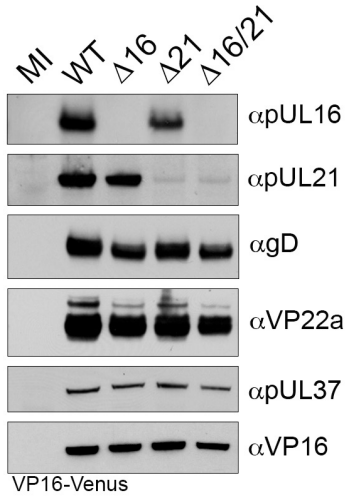

Fig. 2. Expression of HSV-1 polypeptides in infected cells**.** Vero cells were synchronously infected with the indicated viruses or mock infected (MI). Cell lysates were collected 24 h post-infection and analyzed by SDS-PAGE and western blotting with antibodies for HSV-1 proteins. Both pUL16, or pUL21 are only observed in infected cell lysates for viruses expressing the corresponding wild-type gene. Additionally, lysates were probed with antibodies for gD, VP22a, pUL37, and VP16 which are all expressed with early and late gene kinetics and are unaltered in mutant virus lysates. Anti-VP16 antibodies detect the VP16-Venus fusion protein (92 kD).

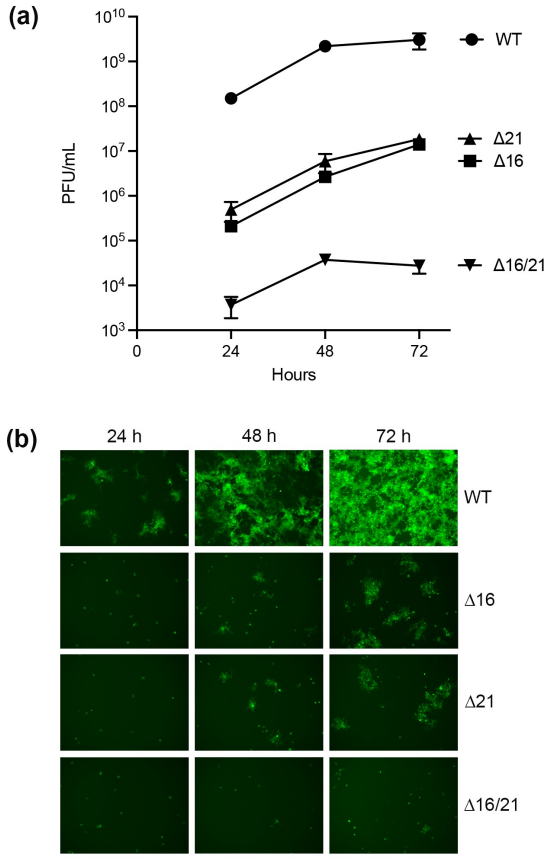

Fig. 3. Viruses encoding deletions in UL16 and UL21 are attenuated for replication in Vero cells. (a) Vero cells were infected with each virus at a multiplicity of infection (MOI) of 0.01 plaque forming units (PFU)/cell and the infected cells harvested every 24 h over a 72 h period. Virus yield (PFU/mL) was enumerated by titration on G5-9 monolayers. Data from replicates was plotted for the multi-step growth curves. (b) Representative images of Vero cells infected at an MOI of 0.01 PFU/cell from the same cultures as above were obtained by fluorescence microscopy to visualize VP16-Venus expression at the different times post-infection.

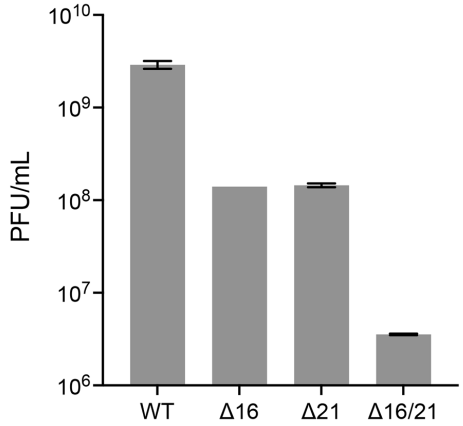

Fig. 4. Single-step growth curves of the mutant viruses. Vero cells were infected at an MOI of 10 PFU/cell and the virus progeny harvested 24 h post-infection. Virus titers were enumerated by plaquing on G5-9 cells. Data presented are representative of two biological replicates.

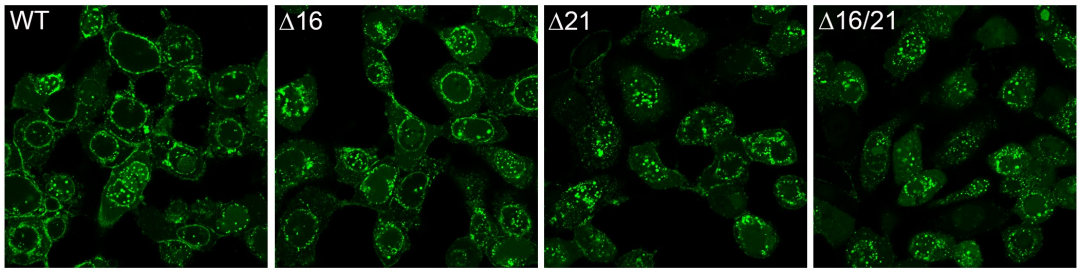

Fig. 5. Confocal microscopy reveals disrupted perinuclear VP16-Venus localization in infected cells lacking pUL21. RPE-1 cells were plated in chamber slides and synchronously infected with each virus for 12 hours prior to live cell imaging by confocal fluorescence microscopy to visualize VP16-Venus (objective 63X). Perinuclear VP16-Venus was observed in WT virus and Δ16 infected cells, but this distribution became irregular in either the Δ21 or Δ16/21 infected cells.

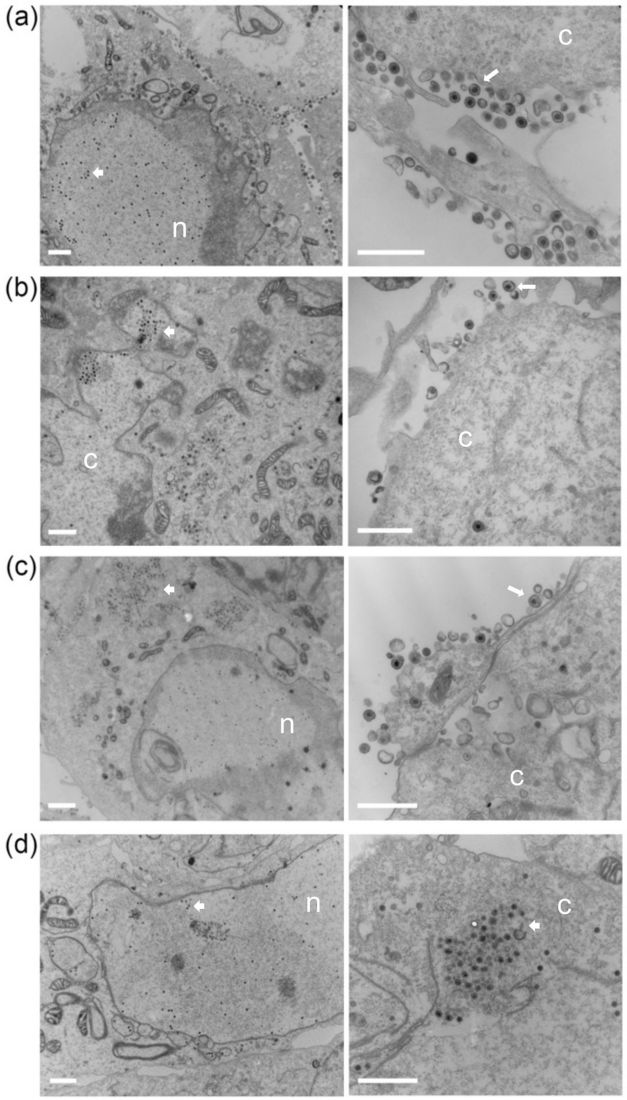

Fig. 6. Transmission electron microscopy shows enveloped capsids in single Δ16 or Δ21 null virus infected cells, but not in Δ16/21 infected cells. Vero cells were synchronously infected with WT (a), Δ16 (b), Δ21 (c), or Δ16/21 (d) viruses (scale bar 1 μm) then fixed 16 h post-infection and processed for TEM imaging. Enveloped virus particles were observed in the cytoplasm and egressing from WT infected cells (white arrows) and observed at a lower frequency in Δ16 or Δ21 infected cells. Enveloped virus particles were not observed in Δ16/21 cells and an accumulation of unenveloped capsids (white arrowheads) was observed in the cytoplasm of these cells. The nucleus (n) and cytoplasm (c) are marked.

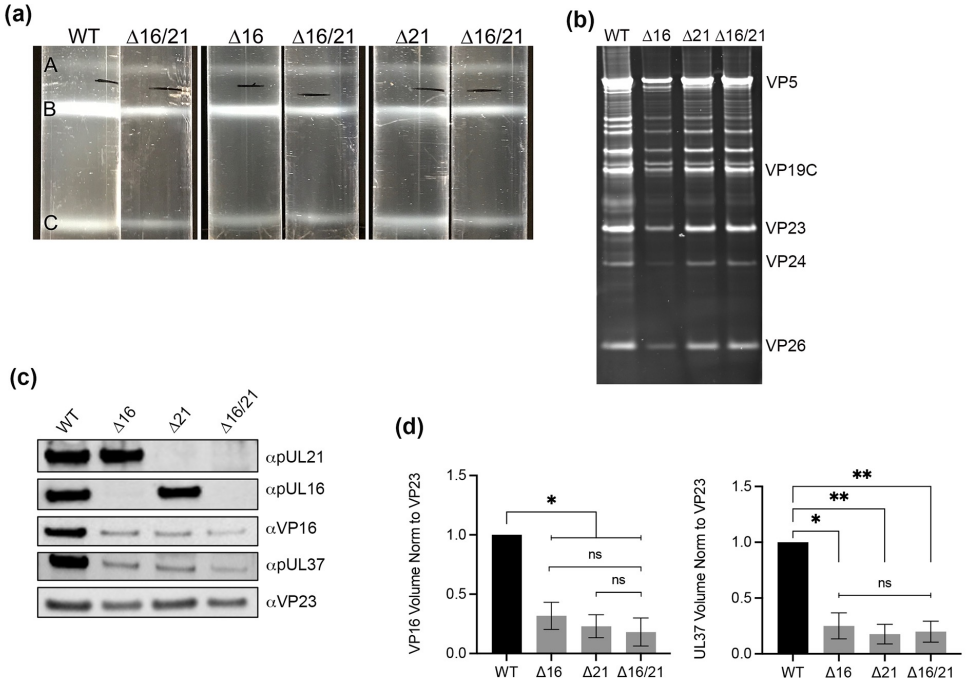

Fig. 7. Isolation and analysis of mutant capsid particles. Vero cells were infected with each virus (MOI=5) and infected cell pellets were collected 24 h post-infection. Capsids from infected cells were released by treating infected cell pellets with 2X CLB and sonication followed by separation of capsids on a 20-50% sucrose gradients and ultracentrifugation. (a) Each capsid form — A, B, and C — are observed as light scattering bands and denoted on the gradient images, each compared to the Δ16/21 capsid bands. (b) C-capsids were harvested by side puncture from each gradient and proteins were separated by SDS-PAGE and observed by Sypro Ruby staining. Visible capsid protein identities are indicated. (c) Proteins from the same C-capsids were again separated by SDS-PAGE and probed for pUL16, or pUL21 by western blotting as well as the capsid triplex protein VP23. Additionally, capsid proteins were also probed for inner-tegument protein pUL37 or outer-tegument protein VP16 (Venus-fusion). (d) Quantitation of levels of VP16 and pUL37 detected in the C-capsid fractions relative to the triplex protein, VP23. Western blots were analyzed using the iBright 1500, yielding values of the Local Background Corrected Volume for each protein band. The VP16 and pUL37 volumes were normalized to the VP23 volumes, and then normalized to the WT capsids. Statistical analyses was performed with GraphPad Prism 9 using Student's *t*-test. ns: not significant, *P*=<0.05 (*,**,***).